Experimental Research on the Stability behavior of Composite Curved Stiffened Fuselage Panel under Four-Point-Bending load

IOP Conf. Series: Materials Science and Engineering **563** (2019) 022005 doi:10.1088/1757-899X/563/2/022005

Experimental Research on the Stability behavior of Composite Curved Stiffened Fuselage Panel under Four-Point-Bending load

C Hao[1], C Y Nan[1], Y Z Bo[2] and L Lei[2]

[1]Aircraft Strength Research Institute of China, Xi'an 710065, China

[2]Shanghai Aircraft Design and Research Institute, Shanghai 201210, China

Corresponding author's E-mail: jjocking@126.com (C Hao)

Abstract. In the design of fuselage structure, not only the longitudinal stability should be considered, but also the circumferential stability of fuselage structure is important because of its circumferential bearing of bending moment, shear force and axial force, as well as considering crash conditions. In this paper, the circumferential stability test researches of the fuselage structure were performed on the single-frame curved panel test specimens. The buckling and post-buckling characteristics of the single-frame curved panel under the negative bending condition were examined by four-point bending loading method. At the same time, the buckling mode, failure process and damage mechanism of single-frame curved panel were analysed through the load-strain curves of the skin and the different degree of damage of the three test specimens. The experimental results show that the buckling of skin is an important factor causing the debonding between the cap-stringers and the skin. The expansion of the debonding area greatly reduces the bearing capacity of the curved stiffened panel structure, which eventually leads to the breakage of the frame.

1.Introduction

Composite materials have been widely used in aerospace industry due to their considerable stiffness, strength-weight ratio and design characteristics. In the past decades, many more effective composite structures, such as composite laminates, honeycomb sandwich structures and three-dimensional braided materials, have begun to replace a large number of metal materials [1-3]. In the research and development of some new civil and military aircraft, all-composite fuselage has been developed. Its structure is similar to that of traditional fuselage, and consists of skin, circumferential partition frame and axial long truss, which is the typical bearing form of fuselage [4-7].

In practical structures, composite stiffened panels are often subjected to axial compressive loads, which can easily lead to structural buckling [8-9]. Moreover, a large number of studies have found that stiffened panels still have a long bearing stage after buckling, which is called post-buckling stage. The post-buckling study of composite stiffened panels can give full play to the bearing advantages of composite structures and further reduce the weight of structures [10-13]. However, up to now, there are no specific guidelines for the post-buckling design of stiffened composite plates. Therefore, it is very important to study the stability behaviour of stiffened plates [14-15].

Composite fuselage is a typical stiffened panel structure, its axial compression stability is a necessary factor for assessment, and the circumferential stability is also very important. The fuselage section is subjected to compressive shear and bending loads along the circumferential direction,

among which the bending load is the most important, which mainly examines the ability of the fuselage section to maintain structural integrity under static or collision conditions. Therefore, it is an important part of fuselage design to study the circumferential stability of fuselage structure and evaluate its instability and failure modes under circumferential bending load [16-18]. The buckling and post-buckling characteristics of single-frame curved panels intercepted from composite fuselage structure under pure bending were studied by four-point bending loading method. The failure modes and failure modes of composite fuselage were discussed through the test results.

2. Experiment

2.1 Specimens

The test specimens used in the test are intercepted from the fuselage section, which are completely consistent with the real structure, including skin, seven cap-stringers and a single frame. Large-scale composite structure is relatively expensive, and only three specimens have been manufactured for testing in this experiment. As shown in Fig. 1, the basic shape of specimen is a curved stiffened panel with a radius of 2960 mm, a span of 28.455 degrees, and a width of 620 mm. All parts of the test specimen are made of IMA/M21E composite material and unidirectional carbon fiber/epoxy prepreg. The thickness of the layer is 0.19 mm and the curing temperature is 180 C. Among them, the skin thickness is 2.28 mm, which is made of 12 layers of the same prepreg, and the stacking sequence is [45/-45/-45/90/45/0]s. The cap-stringer has a height of 31.5 mm and a thickness of 1.71 mm. It has nine layers as follows: [45/0/0/-45/90/-45/0/0/45]. The shear-clip's height is 67 mm, thickness is 2.66 mm, and the number of layers is [45/-45/0/90/-45/45/0/45/-45/90/0/-45/45]. The height of Z-frame web is 80 mm and the width of edge is 28 mm. As shown in Fig. 2, the thickness is 1.9 mm, and the stacking sequence is 45/-45/0/90/45/-45/90/0/-45/45].

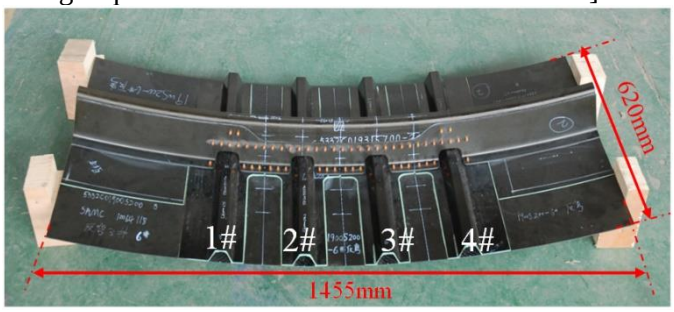

Figure 1. Composite curved stiffened fuselage panel

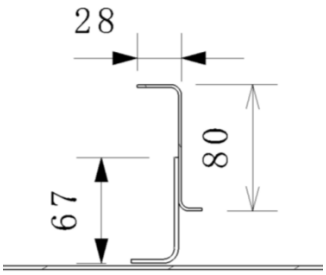

Figure 2. Cross section configuration

2.2 four-point bending test

In this experiment, the negative bending loading of composite fuselage curved panel was carried out on Instron 8804 (500kn) test machine by four-point bending loading technology, as shown in Fig. 3. The curved panel specimen is placed on two support bases of the supporting platform. The compression load is applied by two load bases of the loading platform. Two support bases are inside and two load bases are outside. In order to avoid local damage and instability caused by concentrated load on the loading section of the test specimen, parts such as reinforced frame and plate are designed to reinforce the loading section of the test specimen. The horizontal distance L between the support seat and the bearing seat is 270 mm. If the loading force of the testing machine is F, the bending moment M is F•L/2. In the experiment, displacement loading was used with a loading speed of 1 mm/min. There were 24 strain gauges on each specimen for capturing local strain and identifying buckling mode. All strain gauges were pasted back-to-back, and the direction of 0 degree was circular along the curved panel, as shown in Fig. 4. The strain gauge No. 1-12 is on the inner surface of the skin. The strain measurement system is ST-16 strain acquisition system with a measurement range of (+20000u) and a measurement accuracy of 0.5% FS.

Figure 3. Four-point-bending test device

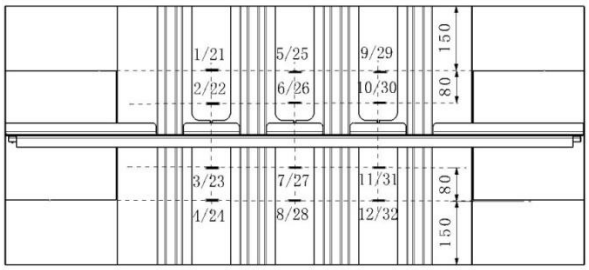

Figure 4. Strengthening components of specimen

3.Results and discussion

3.1 buckling and post-buckling

The load-displacement curves of three test panels are shown in Fig. 5. The buckling, damage and failure process of the specimen can be roughly analysed according to the curves and combining with the sound recording during the test. For Panel 1, when Panel 1 was loaded to 50kN, the first load drop occurred, accompanied by cracking sound. The second load drop occurred at 62kN, accompanied by huge noise and continuous cracking sound, but no obvious signs of damage were found. When the test was loaded to 64kN, the test has been stopped intentionally in order to better detect and study the initial damage location. When Panel 2 was loaded to 60kN, the first load drop occurred, and the decrease was 17%, accompanied by a huge cracking sound. When the load rises back to 60kN, a second small drop occurs, accompanied by a larger noise. When the load continues to load to 71.3KN, the third load drop occurs, accompanied by continuous cracking sound. After that, it is difficult for the load to continue to increase, indicating that the structure was failure. The first load drop of Panel 3 occurred at the level of 66kN, accompanied by a larger cracking sound. The initial damage of Panel 3 is later than that of Panel 1 and Panel 2. However, after the initial damage of Panel 3, repeated downloads and sustained noise appeared, indicating that it has entered a sustained period of destruction. When Panel 3 was loaded to 71.6kN, there was a large drop and loud noise. Stringer 2 and stringer3 of Panel 3 are completely separated from the skin, and the frame was broken, which is shown in Figure 7.

The load-strain curves of the three curved panels obtained from the tests are shown in Fig. 6 to Fig. 8. The stability of the curved panels can be accurately analysed by using the load-strain curves. Fig. 6 shows the load-strain curve of Panel 1. It shows that the initial buckling position is near Gauge 8 of the skin between stringer 2 and stringer 3, that is, the middle skin of the test section. The initial buckling load is about 47.5kN, and the strain in the middle of the skin is -640με. When the load is about 58kN, the second buckling occurs near the Gauge 1 of the skin between stringer 1 and stringer 2, and the buckling strain is about -919με.

Fig. 7 shows the load-strain curve of Panel 2. It can be concluded that the initial buckling of Panel 2 occurs near Gauge 6 of the skin between stringer 2 and stringer 3. The initial buckling load is about 47.5kN, and the strain in the middle of the skin is -665με, which is the same as the initial buckling position, load and strain of Panel 1. When the load is about 58.5kN, the second buckling occurs near Gauge 11 of the skin between stringer 3 and stringer 4, and the buckling strain is about -1121με. Fig. 8 shows the load-strain curve of Panel 3. It can be found that the initial buckling of Panel 3 occurs near Gauge 7 of the skin between stringer 2 and stringer 3, and the surface strain in the skin is -882με. With the increase of loads, the second buckling occurs near the skin Gauge 10 between stringer 3 and stringer 4 at one end of the curved plate at about 63kN, and the buckling strain is about - 1443με.

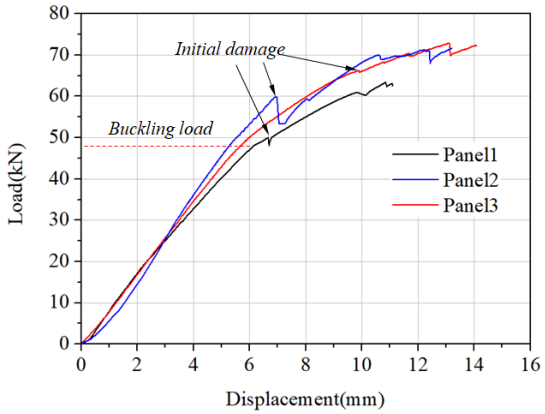

Figure 5. Load-strain curves of panel 1

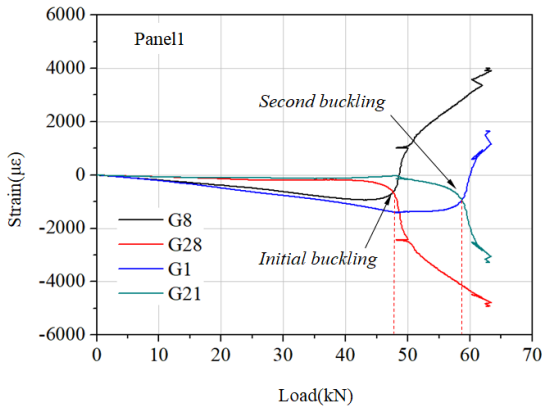

Figure 6. Load-strain curves of panel 2

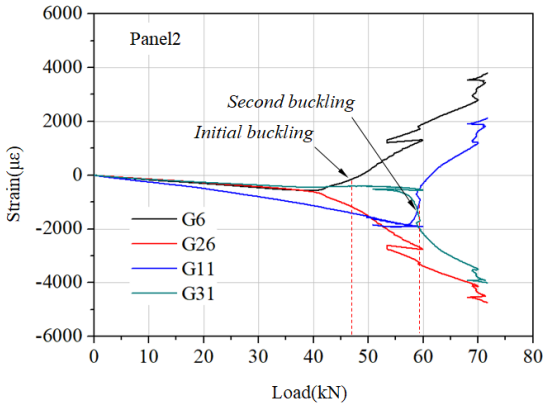

Figure 7. Load-strain curves of panel 3

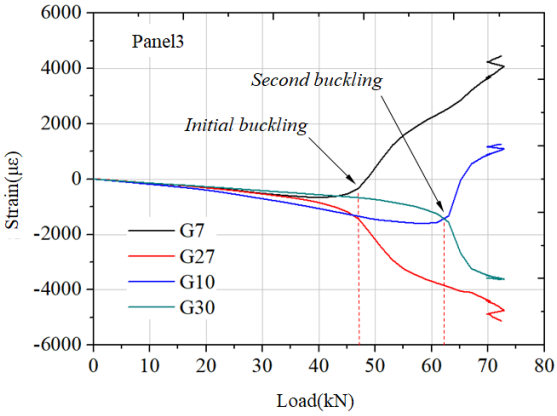

Figure 8. Debonding area of panel 1

3.2 failure mode and process

After the tests, the ultrasonic non-destructive testing (NDT) has been carried out to detect and evaluate the damage of curved panels. Ultrasound A detection method can directly mark the damage location and area on the specimens, and evaluate the damage status of the structure conveniently and intuitively. Fig. 9 is the NDT results of Panel 1. It can be seen from the figure that small areas of debonding appeared at the bottom of stringer 2 and stringer 3 near the middle area of the frame, respectively. The Panel 1 test stopped earlier and the damage degree of the specimen was slight. The damage of Panel 1 can be used as the initial damage mode. The NDT results of Panel 2 are shown in Fig. 10. The graph shows that stringer 3 and the skin are debonded as a whole, and the surrounding skin is delaminated in a large area, and the edges of stringer 2 and stringer 4 are debonded to the skin. The damage of Panel 2 is much more serious than that of Panel 1. The debonding area extends from the stringer at the bottom of the frame to the edge of the skin and adjacent stringer. The NDT results of Panel 3 are shown in Fig. 11. From the graph, the whole stringer 3 debonded from the skin, the stringer 2 and stringer 4 are mostly debonded from the skin, and the high locking bolts connecting shear-clip and skin between stringer 2 and stringer 4 are all pulled out and destroyed.

The damage initiation and propagation paths can be roughly clarified by comparing and analysing the damage conditions of three curved panels. The main type of damage is the debonding of the stringers and the skin. With the increase of load, the buckling of skin becomes more serious, and the debonding area extends from the bottom of frame to the edge of skin, and from middle of stringer to adjacent stringer. At last, a large area of debonding occurs in the middle of the skin, which leads to the overall instability of the skin, and produces a large peeling stress, leading to tensile fracture of the high lock bolt between the connecting frame and the skin, as shown in Fig. 12.

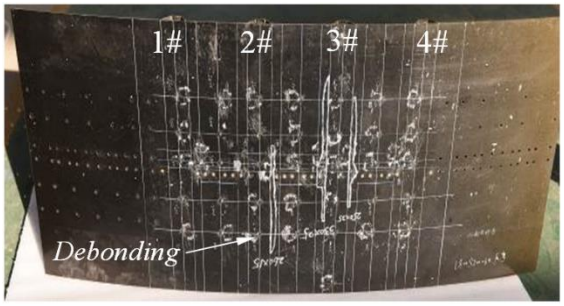

Figure 9. Debonding area of panel 1

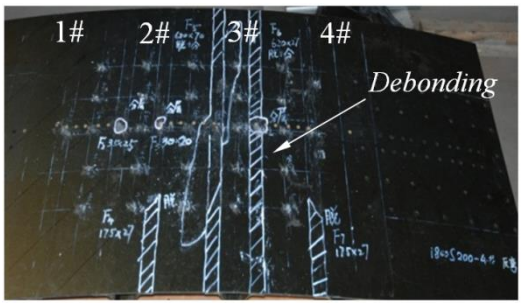

Figure 10. Debonding area of panel 2

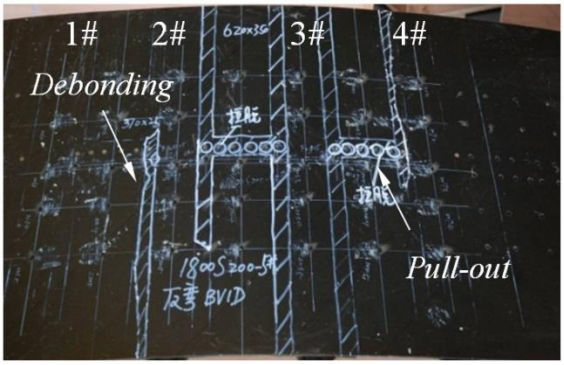

Figure 11. Debonding area of panel 3


Figure 12. The structural failure of panel

4.Conclusion

In this paper, the pure bending test of composite curved stiffened fuselage panel is carried out by four-point bending test technology. The stability behaviour, failure mechanism and process of the panels are analysed and the following conclusions can be drawn:

• The buckling of the skin is an important factor leading to the debonding of stringers and skin. With the expansion of the debonding area, the skin loses the support of the stringers and the overall instability occurs.

• Initial buckling of skin results in debonding damage of stringers. The damage expands with the increase of load, and then causes secondary buckling occurring in the adjacent skin. In this mode, the debonding damage is transmitted from a stringer to a nearby stringer and more stringers.

Acknowledgments

The support of project of composite CSFP come from Shanghai Aircraft Design and Research Institute, as part of the Civil aircraft scientific research project (MJ-2016-F-01), is gratefully acknowledged. The authors wish to thank colleagues for the assist in the test.

References

[1] Gibson R F. A review of recent research on mechanics of multifunctional composite materials and structures. *Composite Structures* 92 (2010) 793-810.

[2] Albert R, Adam P. Vibroacoustic tailoring of a rod-stiffened composite fuselage panel with multidisciplinary considerations. *Journal of aircraft* 52 (2015) 232-241.

[3] Mo Y M, Ge D Y, He B L. Experiment and optimization of the hat-stringer-stiffened composite panels under axial compression. *Composites Part B* 84 (2016) 285-293.

[4] Maher B Z, Tarek L B, Mohamed S. Mechanical response of a hexagonal grid stiffened design of a pressurized cylindrical shell-application to aircraft fuselage. *Thin-Walled Structures* 127 (2018) 40-50.

[5] Albert R A, Adam P K. Vibroacoustic Tailoring of a Rod-Stiffened Composite Fuselage Panel with Multidisciplinary Considerations. *Journal of Aircraft* 52 (2015) 692-702.

[6] ZE L Y, PU X. Crashworthiness Study of Composite Fuselage Section. *Key Engineering Materials* 725 (2016) 94-98.
[7] S.M.O. Tavares, P.M.S.T. de Castro. Stress intensity factor calibration for a longitudinal crack in a fuselage barrel and the bulging effect influence. *Engineering Fracture Mechanics* 78 (2011) 2907-2918.
[8] Jin S J, Xiu G J, Xiang R F. Fracture Analysis for Damaged Aircraft Fuselage Subjected to Blast. *Key Engineering Materials* 348 (2007) 705-708.
[9] A. Murphy, M. Price, C. Lynch, et al. The computational post-buckling analysis of fuselage stiffened panels loaded in shear. *Thin-Walled Structures* 43 (2005) 1455-1474.
[10] John T. W; Clarence C. P, Damodar R. Ambur Residual strength prediction of damaged composite fuselage panel with R-curve method *Composites Science and Technology*, 66 (2006) 2557-2565.
[11] S.Heimbs, M.Hoffmann, M.Waimer, et al. Dynamic testing and modelling of composite fuselage frames and fasteners for aircraft crash simulations. *International Journal of Crashworthiness* 18 (2013) 406-422.
[12] R. sturm, Y. Klett, Ch. Kindervater, et al. Failure of CFRP airframe sandwich panels under crash-relevant loading conditions. *Composite Structures* 112 (2014) 11-21.
[13] Gibson R F. A review of recent research on mechanics of multifunctional composite materials and structures. *Compos Struct* 92 (2010) 2793-810.
[14] Ubertini F, Laflamme S, Ceylan H, et al. Novel nano-composite technologies for dynamic monitoring of structures: a comparison between cement-based embeddable and soft elastomeric surface sensors. *Smart Mater Struct* 23 (2014) 045-023.
[15] Gohardani O, Elola M C, Elizetxea C. Potential and prospective implementation of carbon nanotubes on next generation aircraft and space vehicles: a review of current and expected applications in aerospace sciences. *Prog Aerosp Sci* 70 (2014) 42-68.
[16] Lei Z X, Zhang L W, Liew K M. Free vibration analysis of laminated FG-CNT reinforced composite rectangular plates using the kp-ritz method. *Compos Struct* 127 (2015) 245-59.
[17] Maher B, Tarek L, Mohamed S. Mechanical response of a hexagonal grid stiffened design of a pressurized cylindrical shell-application to aircraft fuselage. *Thin-Walled Structures* 127 (2018) 40-50.
[18] Enrique G M, Luis R T, Rafael C T. Buckling analysis of functionally graded carbon nanotube-reinforced curved panels under axial compression and shear. *Composites Part B* 108 (2017) 243-256.